Synthesis and Characterization of WO_3 Nanowedge for Electrochromic Application

A Thesis Submitted
In Partial Fulfilment of the Requirement
For the degree of

BACHELOR OF TECHNOLOGY
(B. TECH.)

Submitted by:
Rajashree Swain
ROLL NO-111CR0575

Under the Supervision
of
Prof. Debasish Sarkar

DEPARTMENT OF CERAMIC ENGINEERING,
NATIONAL INSTITUTE OF TECHNOLOGY, ROURKELA
MAY 2015

CERTIFICATE

This is certified that the work enclosed in the project entitled "**SYNTHESIS AND CHARACTERIZATION OF WO_3 NANOWEDGE FOR ELECTROCHROMIC APPLICATION**" by Rajashree Swain bearing Roll No. 111CR0575 in partial fulfilment of the requirement of the award of Bachelor of Technology Degree from Department of Ceramic Engineering at National Institute of Technology, Rourkela is an authentic work carried out by her under my extreme guidance and supervision.

To the best of my acquaintance, the work embodied in the thesis has not been submitted to any other university / institute for the award of any Degree or Diploma.

Debasish Sarkar

ASSOCIATE PROFESSOR
Department of Ceramic Engineering
National Institute of Technology
Rourkela-769008

ACKNOWLEDGEMENT

I am heartily grateful to Prof. Debasish Sarkar, Associate Professor Department of Ceramic Engineering, NIT, ROURKELA for his appreciated assistance and supervision in the accomplishment of this project work. I will always remain thankful for his methodical guidance as my instructor.

My deepest thanks to Sangeeta Adhikari for all the indescribable assistance and care she offered.

I also acknowledge all the members of the ceramic engineering department for their recommendations and cooperation during this project work. I would like to express my wholehearted obligations to all my friends who constantly assisted me in the completion of this research project.

Date: 11/May/2015

Rajashree Swain

Roll No.111CR0575

ABSTRACT

Tungsten trioxide is one of the materials that impart multi-functional application in its nanosized form. However, electrochromism is one such application that has been primely researched. Herein, synthesis of nanostructured WO_3 is carried and studied their electrochemical properties. Hydrothermal method has been chosen for the synthesis of hexagonal WO_3 nanowedge. The prime control over hydrothermal duration was performed to understand its influence over crystal structure, crystallinity and phase. With respect to change in hydrothermal duration morphology formation mechanism has been discussed using X-ray diffraction and imaging technique. The present synthesis uses organic compound namely citric acid as the structure directing reagent. FT-IR spectroscopy is analyzed to understand the various structural and functional groups. A simple dip coating of WO_3 nanowedge onto ITO substrate has been used to carry forward the electrochemical properties. These studies illustrated that wedge-like WO_3 nanoparticles prepared in 24 h hydrothermal duration have a hexagonal phase of length ~1.5 μm and of thickness ~320 nm. By means of UV–vis diffuse reflection absorption spectra and BET technique, the optical properties and specific surface area of the hexagonal has been studied. This fabricated electrode exhibits appreciable electrochromic property.

Table of Contents

List of Figures:

Chapter-1

Introduction

1.1. Background and Crystal Structure

Metal oxides in nanostructure form are the key components for various functional material applications especially in the development of smart devices. Tungsten oxides are the special material that has been studied repeatedly for their various capabilities like chromism, photocatalysis and sensing etc. Among the various forms of tungsten oxides, tungsten trioxide (WO_3) is a versatile semiconductor material with a wide band gap ranging from 2.5–3.6 eV, has strong potential for many interesting applications [1]. This WO_3 exists in several polymorphic forms. They are stable within well-defined temperature ranges and transform into each other reversibly. All these forms have structures of the ReO_3 type. The structural form can be described as constructed from (WO_6) octahedra linked by corner-sharing, but they are less symmetrical than ReO_3 owing to distortions of the (WO_6) octahedral [2] .The magnitude of distortion depends on temperature and pure WO_3 go through several structural transformations in accordance to the following sequence: tetragonal → orthorhombic → monoclinic → triclinic → monoclinic as the temperature is lowered from 900℃ to -189^{o}C [3]. Hexagonal tungsten trioxide is an intermediate meta-stable form of WO_3. It is one of the most explored forms due to its one dimensional open-tunnel structure extending through the material and intercalation chemistry [4]. The hexagonal structure of WO_3 is shown in Figure 1. Considering the intercalation chemistry of hexagonal WO_3, there are three possible channels for intercalation of small ions into the crystal structure. They are the triangular tunnels, hexagonal tunnels and four coordinated square windows. This distorted structure provides easy conduction of ions and is a prospective polymorph for applications such as electrochromism, gasochromism, photochromism, sensors and other electro-functional based applications [5, 6].

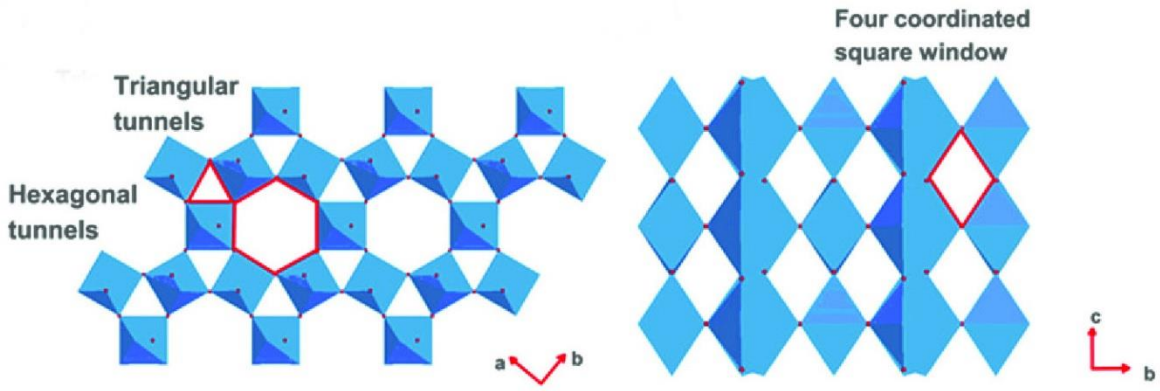

Figure 1. Schematic crystal structure of hexagonal tungsten oxide.

1.2. Electrochromism

Electrochromism is one of the most useful forms of chromism where a material (electrochromic material) can reversibly change its optical properties acquiring a different electronic state by absorbing an electron or by ejecting one by the application of electric voltage. Some of the applications of electrochromism based electrochromic devices (ECD) are active optical filters (e.g. sunglasses), smart windows and mirrors (e.g. darkening a window to control the inlet of sun light displays) and computer data storage [7]. The devices based on WO_3 are on extensive research due to its energy saving property. It takes place from electronic absorption in the visible region followed by switching between the redox states. The color change is mainly varying from a transparent state (bleached) to colored state [8]. One of the prime factors in the electrochromic device is the fabrication of the electrodes. The semiconductor material is coated over transparent conducting glass via different deposition techniques. The transparent conducting oxide (TCO) acts as substrate for deposition of electrochromic material. The substrates are generally Indium doped tin oxide (ITO) and Fluorine doped tin oxide (FTO) coated over glass substrates and were available commercially. The schematic configuration of an electrochromic device is shown in Figure 2.

It consists of an electrolyte that acts as an ion conducting layer, a counter electrode and electrochromic WO_3 layer that is sandwiched between two transparent conductive electrodes [9].

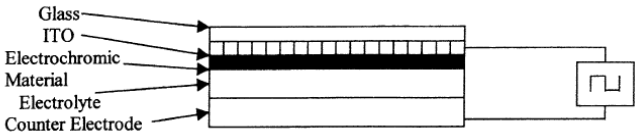

Figure 2. Electrochromic device configuration.

The basic electrochemical reaction as a response of electrochromism is described as equation given below:

$$WO_3 + xM^+ + xe^- \leftrightarrow M_xWO_3 \quad (1)$$

The reaction describes that x amount injection of positive ions occurs as (M^+) along with the equal amount of electrons (e^-). The ions could be typical, M= H, Li and Na and x could be quantified as stoichiometric parameter varying between 0-1 [10]. A typical schematic of working of the electrochromic device has been shown in Figure 3.

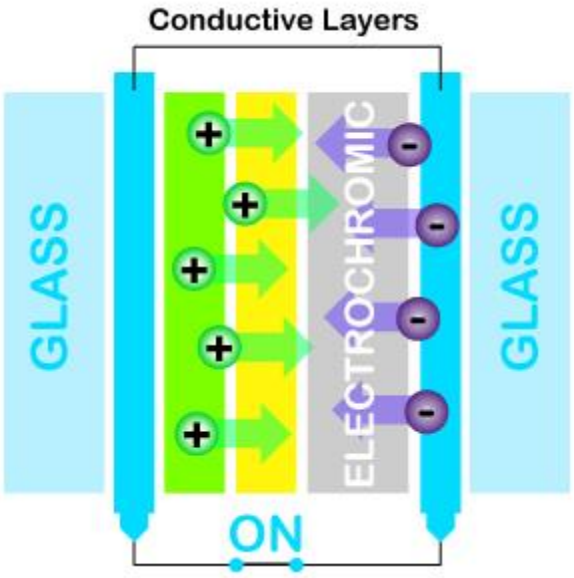

Figure 3. Working of Electrochromic Device.

Chapter-2

Literature Review

Tungsten trioxide is one of the most efficient semiconductor materials for high-performance electrochromism that has been studied since decades. An extensive literature survey has explored that nanosized WO_3 has a high potential for opto-electro-functional applications. The optoelectronic testing is carried using nanostructured films of WO_3 fabricated via various vapor deposition methods that have complicated operations. This lacuna is overcome by fabrication of films by the dip-coating method. This method uses a suspension of WO_3 followed by dipping the substrate in the suspension and drying [11]. This method makes use of nanostructures of WO_3 and can be used for large-scale fabrication of films. The nanostructures of WO_3 are mostly synthesized via different wet chemical methods that include sol-gel, template based, hydrothermal, solvothermal, etc. [12, 13]. Among the methods, the hydrothermal method is a one-step synthesis process to produce different morphology WO_3 nanostructures in the presence of directing agents [14].

Zhang et al. successfully developed monoclinic WO_3 nanoplates via one-step template-free hydrothermal route through a topochemical conversion process. The results depicted that WO_3 nanoplates are about 100–170 nm in length and 30–50 nm in thickness [15]. Another researcher developed WO_3 square nanoplates using organic acids namely L(+)-tartaric acid and citric acid as assistant agents. Hexagonal WO_3 phase was observed in presence of tartaric acid with particle length ~200 nm and thickness ~100 nm whereas orthorhombic phase was developed in presence of citric acid with average particle length ~500 nm and thickness ~100 nm, respectively. The SAED pattern suggests that both of the as prepared WO_3 square nanoplates are single crystalline in nature.

High-performance electrochromism has been observed in porous WO_3 films fabricated by a hydrothermal method using tungsten foils. A transition in phase from hexagonal to

monoclinic was observed after annealing from 400^{o}C to 500^{o}C, respectively. Electrochemical measurements were carried in propylene carbonate solution of 1M lithium perchlorate. The films exhibited high optical modulation with reversibility of 30% and 43.6 cm^2/C^{-1} coloration efficiency. The average particle size observed was 500nm for tree-morphology obtained at 400^{o}C. Hexagonal WO_3 films showed high electrochromism due to large tunnels present in the structure [16].

Recently, Adhikari et al. explored the hierarchical growth of fiber-like hexagonal WO_3 nanostructures. The morphological influencing parameters were amount of structure directing reagent used, time and hydrothermal temperature. Sodium chloride was used as structure directing agent for directional growth of WO3. Almost uniform thickness of WO3 films were achieved through dip-coating onto Indium-doped Tin Oxide (ITO) substrate. A high current density of 8.9 mA/cm^2 was observed [17].

Cai et al. demonstrated a template free solvothermal method for fabrication of nanostructured WO3 array films of about 1.1 micron thickness that showed enhanced electrochromic properties. Nanoarchitectures of WO_3 with vertically aligned hierarchical structures was obtained having stable monoclinic structures. Optical modulation of 66 % at 633 nm with fast switching speed of 4.6s/3.6s and coloration efficiency of 126 cm^2/C^{-1} was observed for the films [18].

Nanorod of WO_3 was developed under a low hydrothermal temperature of 80^{o}C onto W foils. Thermal oxidization at 400^{o}C produced seed layer onto foil. Stable monoclinic crystal phase was developed after 24 h with rod-like morphology having an average particle diameter of 5-10 nm. The WO3 films annealed at 400^{o}C showed the largest optoelectronic contrast with fairly good cycling stability in 0.1 M sulphuric acid as electrolyte [19].

Nanostructured WO_3 cuboid was synthesized using sodium tungstate and fluoroboric acid as structure directing reagent. Phase transformation from metastable hexagonal to monoclinic phase was observed upon varying the molar concentration of the directing reagent. Monoclinic WO_3 nanocuboid was used for electrochemical measurements. Electrode was fabricated using a simple dip coating technique. A fairly good electrochemical response with fast optical modulation was observed [20].

Zheng et al fabricated vertically aligned hexagonal WO_3 onto fluorine-doped tin oxide (FTO) substrate under various pre-treatment of the substrate. Initially, seed coating onto FTO substrates was carried by spin coating tungstic acid colloidal solution prepared by tungstic acid powder and hydrogen peroxide solution. This seed coated FTO substrates were annealed from temperature ranging between 450 to 600^{o}C with varying concentration of the colloidal solution. The annealed substrates were further hydrothermally treated at 170^{o}C for 2 h in the presence of a solution containing oxalic acid, sodium tungstate dihydrate and adjusting pH to 2. Different morphology was observed such as vertical nanorods and spindle-like nanorods. High electrochromic properties were shown by well aligned vertical nanorods due to the high facilitation of Li ions and easy intercalation and deintercalation of ions out the fabricated electrode [21].

Another researcher carried the similar synthesis of WO_3 nanostructures over FTO substrates and their subsequent electrochemical properties were studied. The seed precursor for FTO was prepared by acidification of sodium tungstate dihydrate followed by the addition of hydrogen peroxide to form a stable colloidal solution. The seed was spin coated onto FTO substrate. The hydrothermal process was carried in the presence of acidified solution of sodium tungstate dehydrate to form nanobrick WO_3 thin films. The electrochemical measurements of the fabricated WO3 thin films were carried using 0.5 M lithium perchlorate propylene carbonate electrolyte. Coloration efficiency as observed was calculated to be 39.24

cm^2/C. A high optical modulation was observed with high reversible electrochromism that can contribute towards smart window applications [22].

Su et.al. synthesized nearly monodispersed tungsten trioxide submicrospheres by a facile hydrothermal method using tungsten acid and HCl as the starting materials and thiourea as a structure-directing agent in sodium tungstate dihydrate precursor. They observed that WO_3 submicrosphere was formed following the sequence as rods to spheres with increase in the reaction time. This WO_3 submicrospheres can give enhanced properties relative in the electrochromic devices, gas sensors and photocatalysts. This method can also be practically used to synthesize other spherical oxides such as MoO_3 or MoO_2 in the solution-based approach [23].

In recent, wedge-like nanostructures have been fruitful for the electrochromic application. Thus, in respect of literature survey carried, objectives of the present thesis has been written as follows:

Objective of the Work

- To synthesize WO_3 nanowedge via the hydrothermal method.
- To characterize the synthesized WO_3 nanowedge by various physicochemical techniques.
- To perform electrochemical testing of the fabricated WO_3 nanowedge coated onto ITO electrodes.

Chapter-3

Experimental Procedure

3.1. Synthesis of WO_3 Nanowedge

- Raw materials used:

  Base Precursor: Sodium Tungstate ($Na_2WO_4.2H_2O$)

  Structure directing reagent: Citric acid ($C_6H_8O_7.H_2O$).

The hydrothermal precursor was prepared by dissolving stoichiometric ratio of base precursor, $Na_2WO_4.2H_2O$ as tungsten source and citric acid in 25 ml of distilled water taken in a beaker. The solution was allowed for magnetic stirring for 30 min to completely dissolve the above chemicals. The pH of the solution was reduced to 1 by adding several drops of concentrated 12M HCl to form turbid yellowish solution. After 30 min stirring, the turbid solution was transferred into a 50 ml Teflon-lined stainless steel autoclave, which was processed at 180℃ for varying time duration in a hot air oven. After prerequisite time, the hydrothermal vessel is allowed to cool to room temperature. A typical hydrothermal vessel is shown in Figure 4. The resulting precipitate after reaction was separated by filtering, washing with distilled water to remove the remaining ions, and finally drying at 100^{o}C in air for 12hrs. Flowchart of the reaction is shown in Figure 5.

Figure 4. The image of Hydrothermal Vessel.

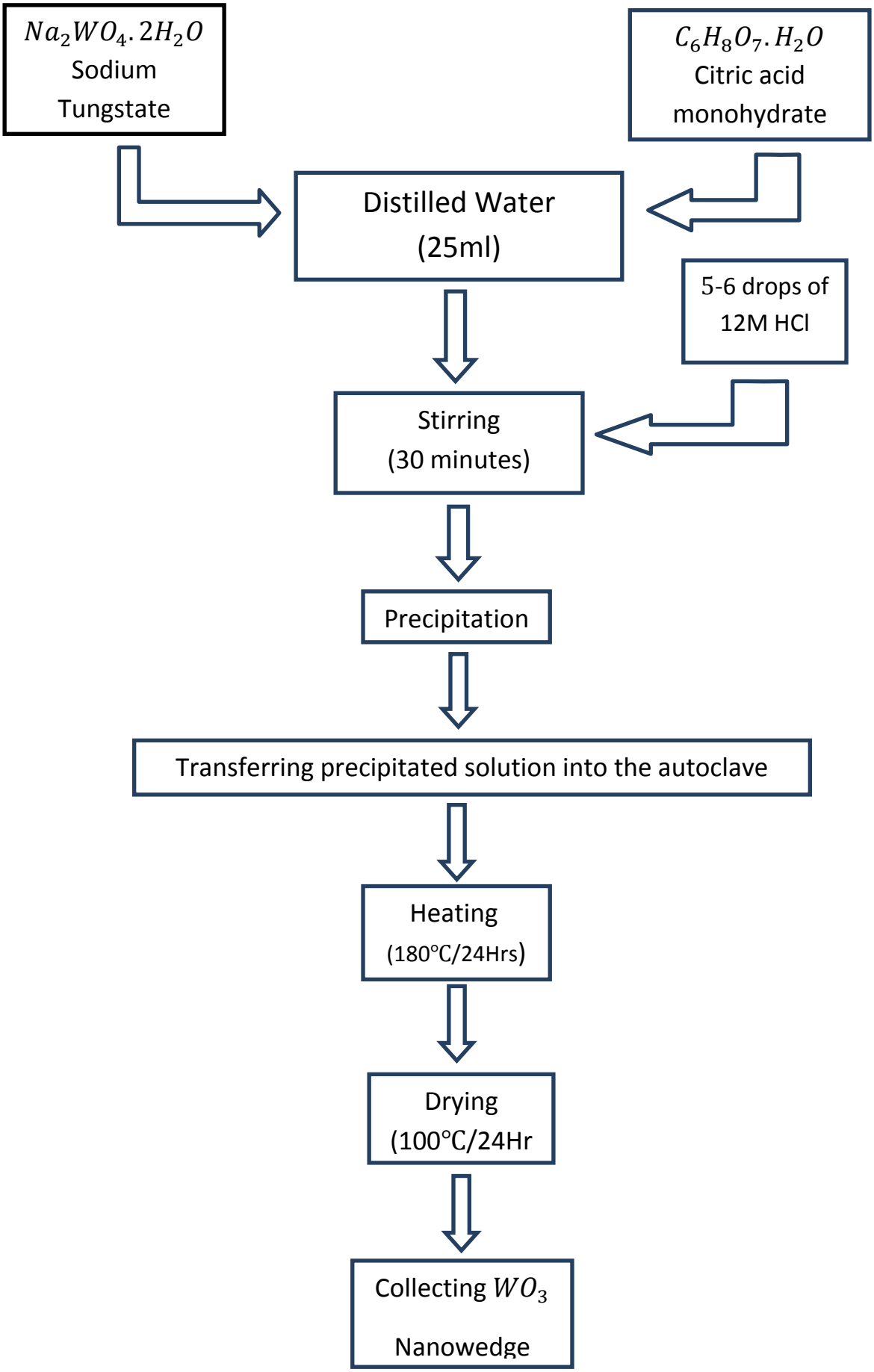

Figure 5. Flowchart for synthesis of WO_3 Nanowedge

3.2. Analytical Characterizations

3.2.1. X-ray diffraction (XRD)

XRD is a rapid analytical and non-destructive instrumental technique that relies on X-rays to study the structure of crystalline materials. In this technique, X-Ray beams are focused on materials with regular three-dimensional repeating structures (i.e. crystalline), where part of the beam is refracted, part is absorbed by the sample material, part is transmitted, part is diffracted and rest are scattered. In this method we can determine the size of crystalline particles. Too small broadening is seen for large sized crystallites while for small sized crystallites, peaks are wider. Scherrer equation determines the crystallite size. Rigaku Ultima IV X-ray diffractometer (Figure 6) has been used for obtaining the XRD patterns.

Figure 6. The image of Rigaku Ultima IV X-Ray Diffractometer.

3.2.2. Field Emission Scanning Electron Microscopy (FESEM)

Field emission scanning electron microscope is a non-destructive versatile technique used to obtain detailed high resolution and long depth of field images of the sample and near surfaces quickly. This technique is used for various applications including dimensional analysis, failure analysis, process characterization, particle identification and reverse engineering. Here

in this experiment, this technique is used for identification of particle sizes and dimensions of different samples. Figure 7 shows the digital image of NOVA NANOSEM FEI 450 system.

Figure 7. Digital image of NOVA NANOSEM FEI 450 system.

3.2.3. Brunauer–Emmett-Teller (BET) Analysis

This is a fully automated analysis technique relying on Brunauer–Emmett-Teller (BET) theory which explains the physical adsorption of gas molecules (nitrogen) on a solid surface (sample surface) to determine precise specific surface area of sample material by amounting adsorbed nitrogen multilayer as a function of relative pressure . This technique is used for characterisation of disperse, macroporous materials (pore diameter >50nm), mesoporous materials (pore diameter between 2-50nm) and microporous materials (pore diameter <2nm). The typical BET set up is shown in Figure 8.

Figure 8. BET apparatus for measuring surface area.

3.2.4. Fourier Transform-Infra Red Spectroscopy (FTIR)

The presence of different functional groups was analyzed using FTIR spectroscopy method using Perkin Elmer FTIR spectrophotometer. This measurement uses small pellets prepared using KBr as reference material. A mixture of KBr and the optimized powder is prepared by grinding the powders using mortar and pestle. The homogeneously mixed powder is then pelletized using pelletizer under 3-ton pressure. The image of the instrument is given in Figure 9.

Figure 9. Image of Perkin Elmer FT-IR spectrophotometer.

3.2.5. UV-Diffuse Reflectance

Shimadzu UV-2450 Spectrophotometer was used for measuring the diffuse reflectance of the optimized powders as shown in Figure 10. The diffuse reflectance was measured using barium sulfate as reference material. The measured data occurs due to excitation from ground to excited state in a material when light falls on the material.

Figure 10. The image of Shimadzu UV-Visible Spectrophotometer.

3.3. Electrode Fabrication and Electrochemical measurements

A stable suspension of WO_3 nanowedge in ethanol was prepared using the optimized WO_3 powder. High-frequency ultrasonication was performed for high homogeneous suspension. Indium doped tin oxide (ITO) was used as TCO substrates for coating having electrode dimension 1 cm^2. The clean substrates were dipped into the WO_3 suspension flowed by drying at 60^oC in a hot air oven. The dried substrates were investigated for electrochemical measurements. Biologic science instruments SP-50 (Figure 11) was used consisting of three electrode set up with Platinum as a counter electrode, Ag/AgCl as reference electrode and fabricated WO_3 films as the working electrode. 1M H_2SO_4 was taken as the working electrolyte.

Figure 11. The image of Biologic Science Electrochemical Instrument.

Chapter-4

Results &

Discussion

4.1. X-Ray D iffraction Analysis

The presence of phases and crystallinity is understood using the x-ray diffraction technique. Figure 12 shows the composite x-ray diffraction patterns of the powders synthesized using sodium tungstate and citric acid with variation in hydrothermal time duration for 8 h, 12 h, 16 h, 20 h and 24 h, respectively. The XRD pattern of the powders obtained at 8 h duration showed the presence of both monoclinic and hexagonal crystal phases. The monoclinic phase well matches with the standard JCPDS No. 43-1035 whereas hexagonal phase matches with JCPDS No. 75-2187. The monoclinic peaks are marked as "*". Increasing the duration to 12 h shows a significant increase in (200) plane that suggests formation of hexagonal phase. This plane shows a continuous increase with simultaneous formation of (001) plane till 20 h. A gradual decrease in monoclinic phase is observed till 20 h whereas complete formation of pure hexagonal phase takes place at 24 h with no trace of monoclinic crystal phase.

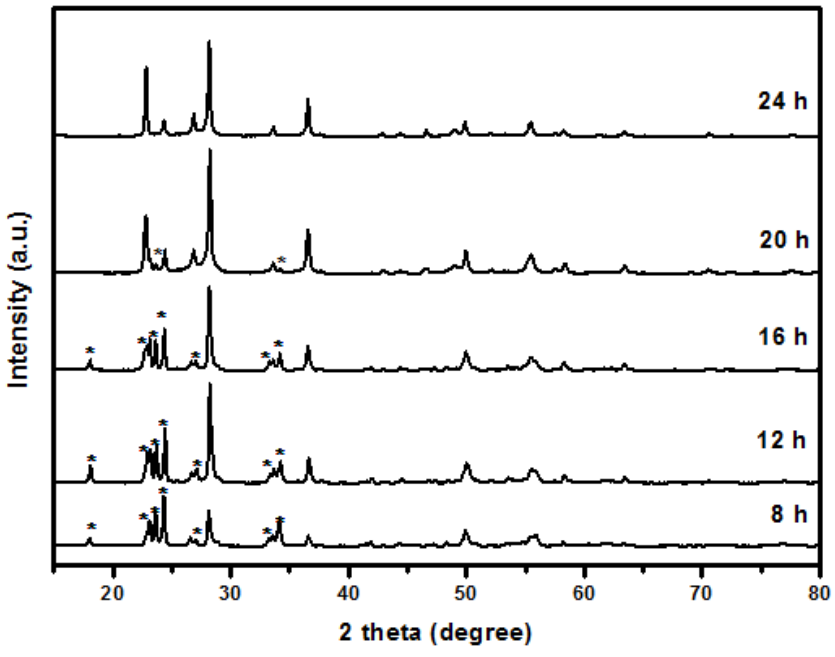

Figure 12. Composite XRD pattern under different hydrothermal duration.

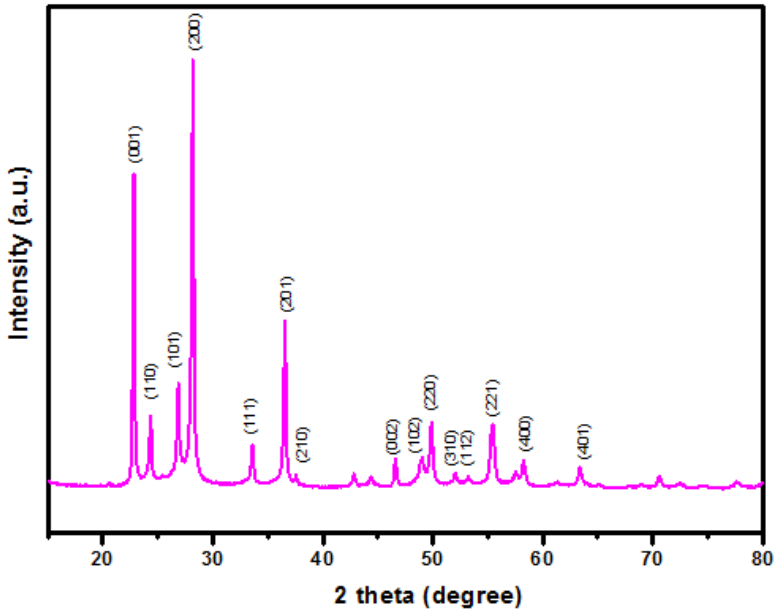

Figure 13 XRD pattern of hexagonal WO_3 nanowedge.

A complete XRD pattern with indexing of planes has been shown in Figure 13. The planes indexed are (001), (110), (101), (200), (111), (201), (210), (002), (102), (200), (310), (112), (221), (400) and (401) corresponds to hexagonal crystal phase.

4.2. Structural Analysis

Structural and functional group present in the crystal structure could be understood from IR spectrum analysis. Figure 14 shows the FT-IR spectra of the WO_3 nanowedge obtained at 24 h hydrothermal duration. Higher wavenumber peak at 3415.25 cm^{-1} attributes to the symmetric vibration of surface water that is loosely bonded with crystal structure through hydrogen bond. The peak at 2360.18 cm^{-1} informs the presence of hydrated water molecules coming from the initial precursor. Moreover, the sharp peak at 1640.05 cm^{-1} is due to symmetric stretching of O-H bond where as peak at wavenumber 1394.12 cm-1 attributes to asymmetric vibration. The peak at 810.84 cm^{-1} at lower frequency is the result of

stretching vibrations of W-O-W bond. These results obtained from this IR spectra analysis support the formation of tungsten trioxide nanoparticles with some water molecule adsorbed in hydroxyl forms [24].

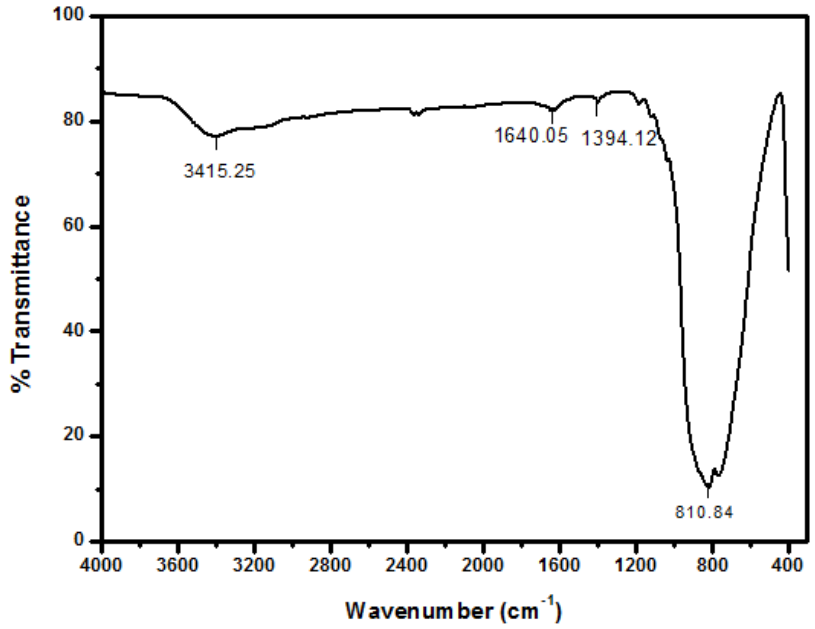

Figure 14. FT-IR Spectrum of optimized WO_3 nanowedge.

4.3. Morphological Analysis

High resolution detailed FESEM images of WO_3 nanopowders synthesized at different hydrothermal duration has been shown in Figure 15 and Figure 16, respectively. Figure 15 (a) shows the image obtained at 8 h duration. Highly agglomerated uniform small plate-like particles forming bundle is seen. The average particle size of this small particle is found to be 167 nm. Upon increasing the hydrothermal duration to 12 h (Figure 15 (b)), non-homogeneous and non-uniform particles are seen with mixture of both small and big plate-like particles. This calculated average particle size is 233 nm. Figure 15 (c) shows decrease in non-uniformity with growth of particles having average particle size of 205 nm for powder synthesized at 16 h. However, uniform sized particle is observed for the 20 h synthesized

WO_3 nanopowders as presented in Figure 15 (d). Distinct plate-like particles having average particle size 500 nm is observed but presence of monoclinic phase as slight impurity in XRD is also observed. Particles are fully grown showing wedge-like morphology for powder synthesized at 24 h. However, particles are agglomerated but there is high connectivity and phase purity among particles as seen in Figure 16 (a). The high resolution FESEM images are shown in Figure 16 (b). The average particle size as calculated has thickness of 320 nm with varied width and length $1.5\mu m$ and specific surface area is observed as $6.89 m^2/g$. The formation of particles followed the sequence of small plate to wedge.

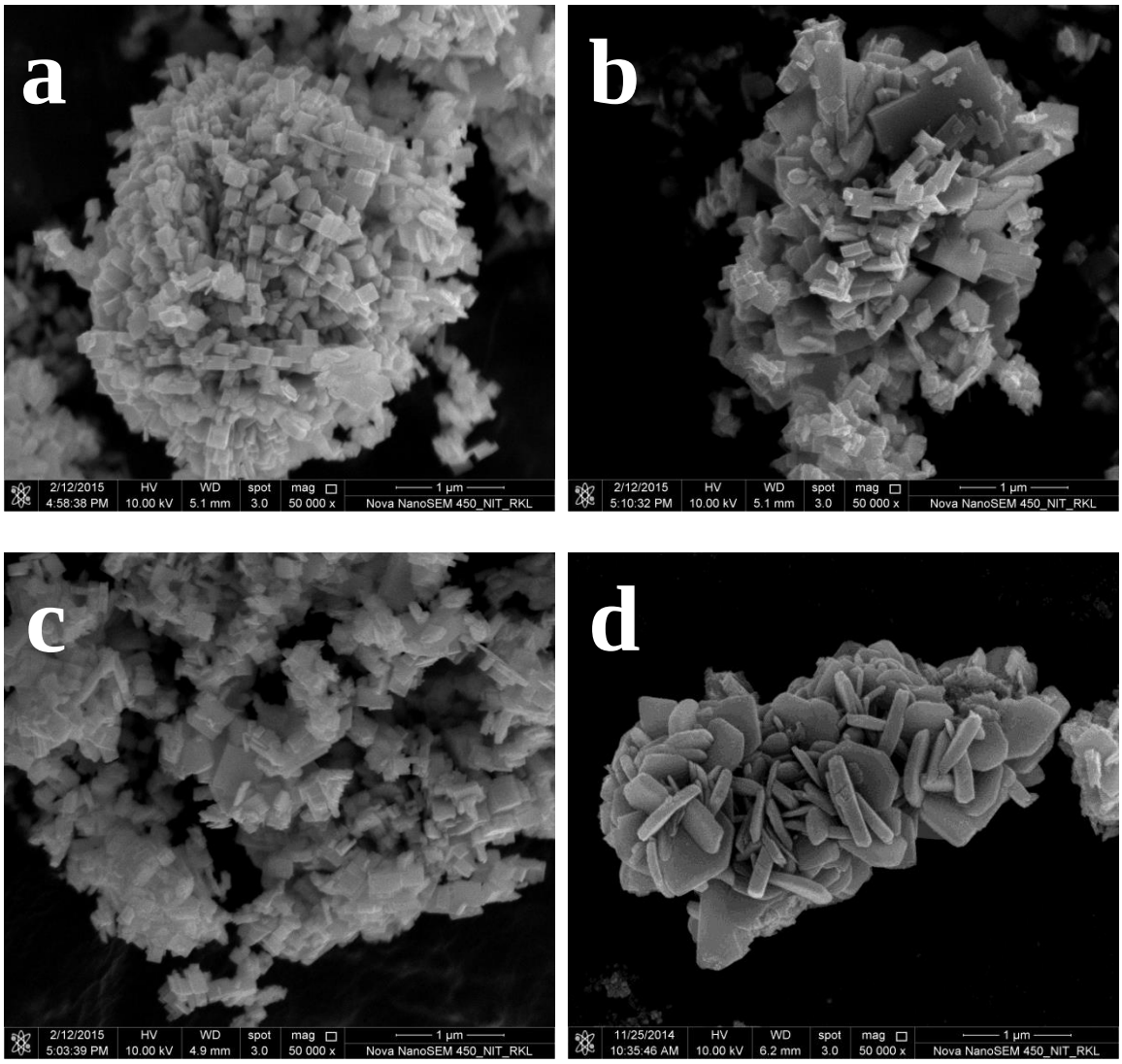

Figure 15. FESEM images of WO_3 nanopowders synthesized at duration (a) 8 h, (b) 12 h, (c) 16 h and (d) 20 h.

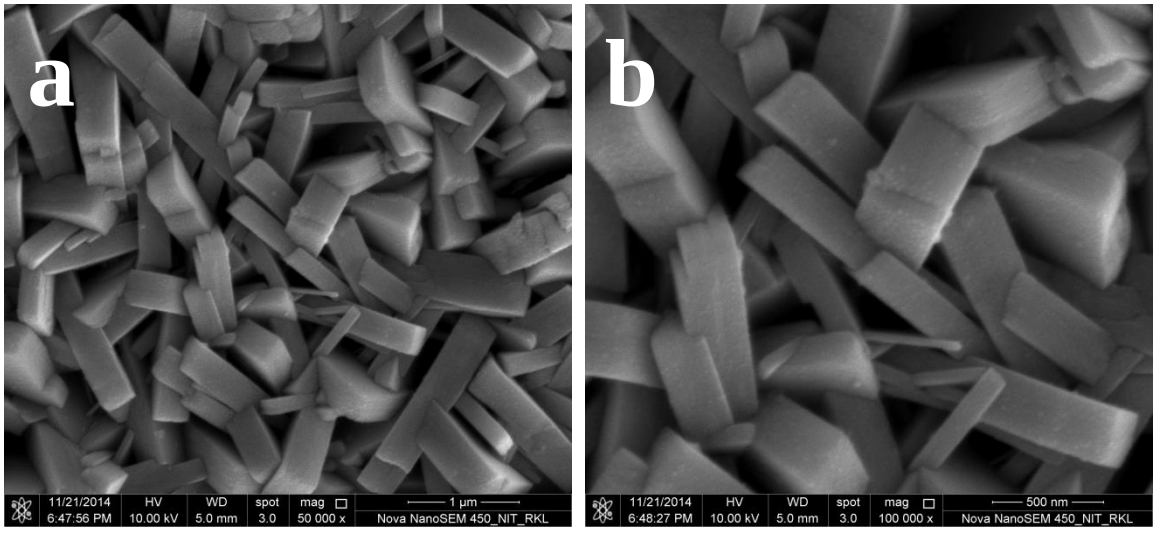

Figure 16. (a) Low resolution and (b) High-resolution FESEM images of WO_3 nanowedge synthesized at 24 h hydrothermal duration.

4.4. UV-DRS and Band Gap determination

UV-vis diffuse reflectance spectra are used to measure the band gap energy of the chosen sample. Figure 17 (a) shows the measured diffuse reflectance spectra that have been used for the estimation of band-gap energy. Figure 17 (b) presents the Tauc Plot. Tauc plot gives the band gap energy which is the square root of the Kubelka–Munk function multiplied by the photon energy and plotted against the photon energy ($E_{photon} = h\upsilon$). This Kubelka–Munk unit of absorption is calculated from the following equation:

$KMU = (1-R)^2/2R$, where R = reflectance (2)

The band gap calculated using the above equation is found to be 2.39 eV that matches with the existing literature value [25, 26].

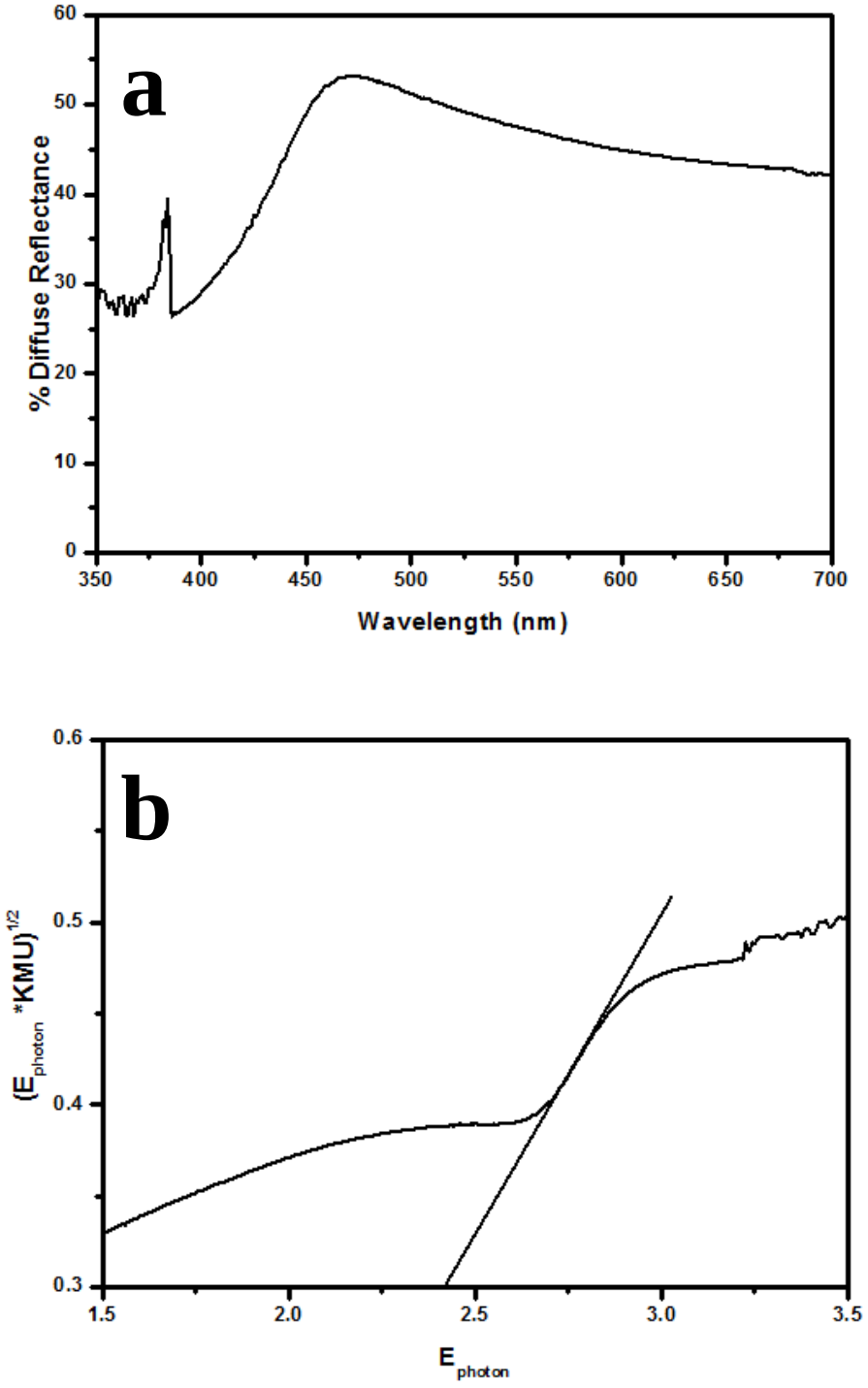

Figure 17. (a) UV-Vis Diffuse Reflectance Plot and (b) Tauc plot for determination of band gap energy.

4.5. Cyclic Voltammetry

Cyclic voltammetry is conducted using three electrode cell configurations where WO_3 coated ITO electrode act as working electrode in 1M H_2SO_4 electrolyte. The potential is allowed to sweep between -0.5 V to 0.5 V with scanning speed 100 mV/s and cyclic voltammogram was obtained as a result of the electrochemical response. During the potential sweep, a reversible color change mechanism is seen. Initially, the electrode fabricated was semi-transparent in nature but during electrochemical reduction, an electrode is colored to blue that is represented as coloration process. However, during oxidation the blue color reversibly changes to its initial form corresponded as bleaching. The blue colouration is attributed to the formation of tungsten bronze. The complete electrochemical reaction for this system is written as:

$$WO_3 \text{ (semi transparent)} + x\mathrm{H}^+ + x\mathrm{e}^- \longleftrightarrow \mathrm{H}_x\mathrm{WO}_3 \text{ (blue)} \quad (3)$$

The current density is obtained as 1.2 mA/cm^2 for WO_3 coated ITO electrode. It is due to high structural openness in the hexagonal structure, the current density is fairly high [27].

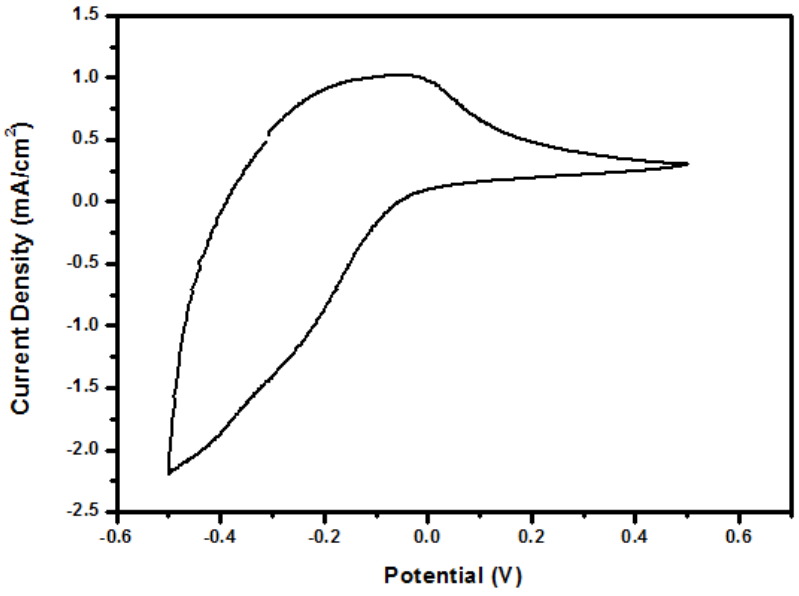

Figure 18. Cyclic Voltammograms of WO_3 nanowedge coated ITO electrode.

Chapter-5
Conclusion

Summarizing the work carried, hexagonal WO_3 nanowedges were successfully synthesized by single step hydrothermal method using sodium tungstate as base precursor and citric acid as structure directing reagent. Influence of hydrothermal duration over the synthesis was carried with of 4 h till 24 h at a constant temperature of 180^oC. Pure hexagonal phase with wedge-like structure was obtained at 24 h hydrothermal duration. The average wedge size as calculated from FESEM image and found to be 320 nm thick and 1.5μm length with varying width. FT-IR spectral analysis confirmed the functioanl groups for WO_3 nanopowders. From UV-vis diffuse reflectance spectra, the band gap energy was found to be 2.39 eV. A fairly high current density of 1.2 mA/cm^2 was observed with coloration and bleaching of the dip coated WO_3 electrodes during electrochemical reaction. These results demonstrate that hexagonal-WO_3 nanowedge has huge potential application in electrochromic devices.

REFERENCES

[1] M. Gillet ,K. Aguir , C. Lemire, E.Gillet, K. Schierbaum, Thin Solid Films 23, 2004, 467.

[2] A. Polaczek, M. Pekala, Z. Obuszko, J. Phys. Condens. Mater, 6, 1994 , 7909 .

[3] P. Roussel, P. Labbe, D. Groult, Acta. Crystallogr. B 56, 2000, 377.

[4] M. Yang , N. K. Shrestha , P. Schmuki, Electrochem. Commun. 11, 2009, 1908 .

[5] X. Fang, Y. Bando, U. K. Gautam, C. Ye and D. Golberg J. Mater. Chem, 18, 2008, 509.

[6] A N Banerjee, Nanotechnology, Science and Applications, 4, 2011, 4.

[7] S. Balaji , Y. Djaoued, A. S. Albert, R. Z. Ferguson, R. Bruning, Chem. Mater. 21, 2009, 1381.

[8] P.Camurlu. RSC Adv., 4, 2014, 55832-55845.

[9] X. Zhang, L. Su, Q. Li, Z. Lu and J. Zuhong, J. Appl. Phys. 38, 1999, 770.

[10] G.Kavei and A.Kavei, Technical and Physical Problems of Engineering, 7, 2015, 22.

[11] K. Tanuj Sapraa and Hagan Bayley Sci Rep. 2, 2012, 848.

[12] M. M. Arafat , B. Dinan , S. A. Akbar and A. S. M. A. Haseeb, Sensors,12,2012, 7207.

[13] O. V. Kharissova, B. I. Kharisov, T. H. García, Synthesis and Reactivity in Inorganic, Metal-Organic, and Nano-Metal Chemistry , 39 (10), 2009, 662.

[14] Y. Wicaksana, S. Liu, J. Scott and R. Amal, Molecules, 19, 2014, 17747.

[15] E.S. Toberer and R. Seshadri, Chem Commun (Camb). 30, 2006, 3159.

[16] S. Adhikari, D. Sarkar, Electrochimica Acta 138, 2014, 115.

[17] Y. E.X. Zhou & Q. I. LiMin, Sci China Chem. 57, 2014, 58.

[18] S. Adhikari and D. Sarkar, Journal of the Electrochemical Society, 162(1), 2015, 1.

[19] H. Zhitao, L. Sisi, L. Junjun, C. Jinkui, and Chen Yong, Semiconductors, 34, 2013, 7.

[20] S. Adhikari and D. Sarkar, ISRN Nanotechnology, 2013.

[21] S. Bai, K. Zhang, X. Shu, S. Chen, R. Luo, D. Li and A. Chen, Cryst Eng Comm, 16, 2014, 10210.

[22] M. Y. Gou, A. M. C. Ng, F. Z. Liu, Y. H. Leung; K. K. Wong, A.Ng, Y. H Ng, W. Gang, A. B. Djurisic., W.K.Chan, 8626, 2013, DOI: 10.1117/12.200297

[23] C. E. Nanayakkara, J. Pettibone and V. H. Grassian, Chem. Chem. Phys, 14, 2012, 6957–6966.

[24] C. Santato, M. Odziemkowski, M. Ulmann, J. Augustynski, J. Am. Chem. Soc., 123, 2001, 10693.

[25] B. Yang, Y. Zhang, E. Drabarek, P. R. F. Barnes, V. Luca, Mater. Chem., 19, 2007, 5664.

[26] M. A. Butler, J. Appl. Phys., 84, 1977, 1914.

[27] M. Regraguia, M. Addoua, A. Outzourhitc, E. E. Idrissia, A. Kachouanea, A. Bougrinea, Sol. Energy. Mat., 77, 2003, 341.